

INTRODUCTION

Mushroom body is the central neuropil structure in the protocerebrum of the locust brain. This structure has been investigated for roles in olfactory coding and associative learning. It is found to be a potential site for the formation of memory traces during olfactory learning.

In the locust's olfactory pathway, the Olfactory Receptor Neurons (ORNs) are the first order neurons in the antennae, which encounter olfactory signals from the environment. ORNs synapse onto the Projection Neurons (PNs) and Local Neurons (LNs) in the Antennal Lobe (AL). PNs receive input from the antennal lobe and send output to the calyx of the Mushroom Body (MB). PNs have their soma located in the antennal lobe and it has been shown that they send branches to the calyx which further project on to the Lateral Protocerebral Lobe (LPL) where they synapse with Lateral Horn Neurons I (LHNI).

MB consists of a calyx neuropil, situated dorso-posterally in the protocerebrum, which is confluent with a forward projecting pedunculus which anteriorly divides into a dorsal lobe extending upwards, and into the medial lobe that extends towards the midline. The matrix of MB consists of ensembles of neurons called Kenyon cells (KC's) which are derived from globuli cells situated above calyx. There are about 50,000 KC's present in a locust MB. Each PN is known to synapse with nearly 50 % of the Kenyon cells.

Kenyon cells, the intrinsic neurons of the mushroom body, receive olfactory input directly from PNs through small neurites located in the calyx region. Any given PN shows abundant activity in response to odors with dense patterns of spikes, while KC's are nearly silent at rest. They respond selectively to odors, with very few spikes. Their soma are located superficially to the calyx. KC's project to the lobes of the mushroom body, where they synapse onto several types of cells, including β Lobe Neurons (β LN's).

Previous work has identified two distinct classes of β LN's: Type I (β LNI) and Type II (β LNII). Only a single β LNI is known to be present for each B Lobe in each hemisphere. It receives direct input from KC's in the β Lobe. Its soma is located in the midline of α and β Lobes. It shows reliable EPSPs after brief stimulation of KC's. About 12-15 cells of β LNII have been identified. They have their soma located in the Lateral Protocerebral Lobe (LPL) and neurites in the calyx, α and β Lobes.

It is known that the neurites of β LNII in α and β lobes receive input from KC's. But it is not clearly known if the neurites of β LNII in the calyx of MB receive or send feedback to the calyx. Previous studies have shown that activity in β LNII is silenced by blocking KC's completely.

Previous studies have shown that the synapse made by KC onto downstream targets exhibits Hebbian Spike Timing Dependent Plasticity (STDP) phenomenon. This STDP enhances the synchronization of the KC's targets and thus helps to preserve the propagation of odor specific codes through the olfactory system.

A single Giant GABAergic Neuron (GGN) is present in each mushroom body which has extensive overlaps with KC projections. It releases the neurotransmitter GABA. It responds to odors in a graded fashion. It receives direct input from KC in the α Lobe and is known to send feedback to the calyx, which is partly understood. GGN shunts the odor-induced synaptic currents by increasing the conductance in KC's.

GABA – positive to GABA- positive	GABA – positive to GABA- negative	GABA – negative to GABA- positive	GABA – negative to GABA- negative
Two GABAergic LN's (AL)	LN's \rightarrow PN's (AL)	ORN's \rightarrow LN's (AL)	ORN's \rightarrow PN's
	GGN \rightarrow KC (MB calyx, Laurent et al, 2011)	KC \rightarrow GGN (α -lobe, Laurent et al, 2011)	PN's \rightarrow KC's (Calyx)
		KC \rightarrow β LNII (β Lobe, Nitin Gupta, Mark Stopfer 2014)	PN's \rightarrow LHNI (LPL, Nitin Gupta, Mark Stopfer 2012)
			KC \rightarrow GABA negative β LNII (β Lobe, Nitin Gupta, Mark Stopfer 2014)
			KC \rightarrow β LNII (β Lobe, Nitin Gupta, Mark Stopfer 2014)

Table 1. Types of Connections in MB network

List of Synapses in MB network:

- | | |
|--|---|
| i. ORNs \rightarrow PNs | ix. KC's \rightarrow β LNII |
| ii. ORNs \rightarrow LNs | x. GGN \rightarrow KC's |
| iii. LNs \rightarrow PNs | xi. GGN \rightarrow α Lobe |
| iv. PN \rightarrow KC | xii. GGN \rightarrow LH |
| v. PN \rightarrow LHNI | xiii. β LNI \rightarrow LH |
| vi. LHNI \rightarrow KC | xiv. β LNII \rightarrow α Lobe |
| vii. KC's \rightarrow α lobe Neuron | xv. β LNII \rightarrow β Lobe |
| viii. KC's \rightarrow β LNI | xvi. β LNII \rightarrow Calyx |

Table 2. Types of Synapses observed in MB network

Excitatory	Inhibitory	Unknown
ORNs \rightarrow PNs	LNs \rightarrow PNs	LHNI \rightarrow KC
ORNs \rightarrow LNs	GGN \rightarrow KC's (in calyx)	
PN \rightarrow KC	GGN \rightarrow LH	
PN \rightarrow LHNI		
KC's \rightarrow α lobe		
KC's \rightarrow β LNI		
KC's \rightarrow β LNII		
KC's \rightarrow GGN (in α lobe)		

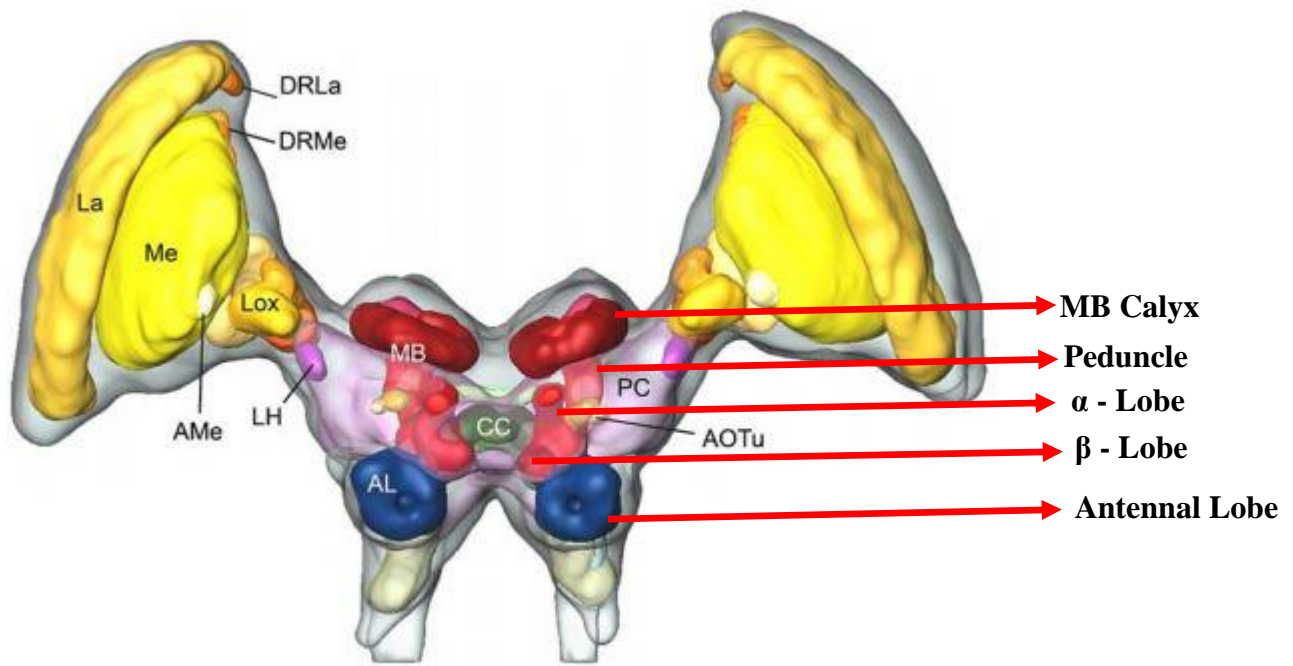


Fig 1. Posterior View of an individual locust brain (Angela et al 2008)

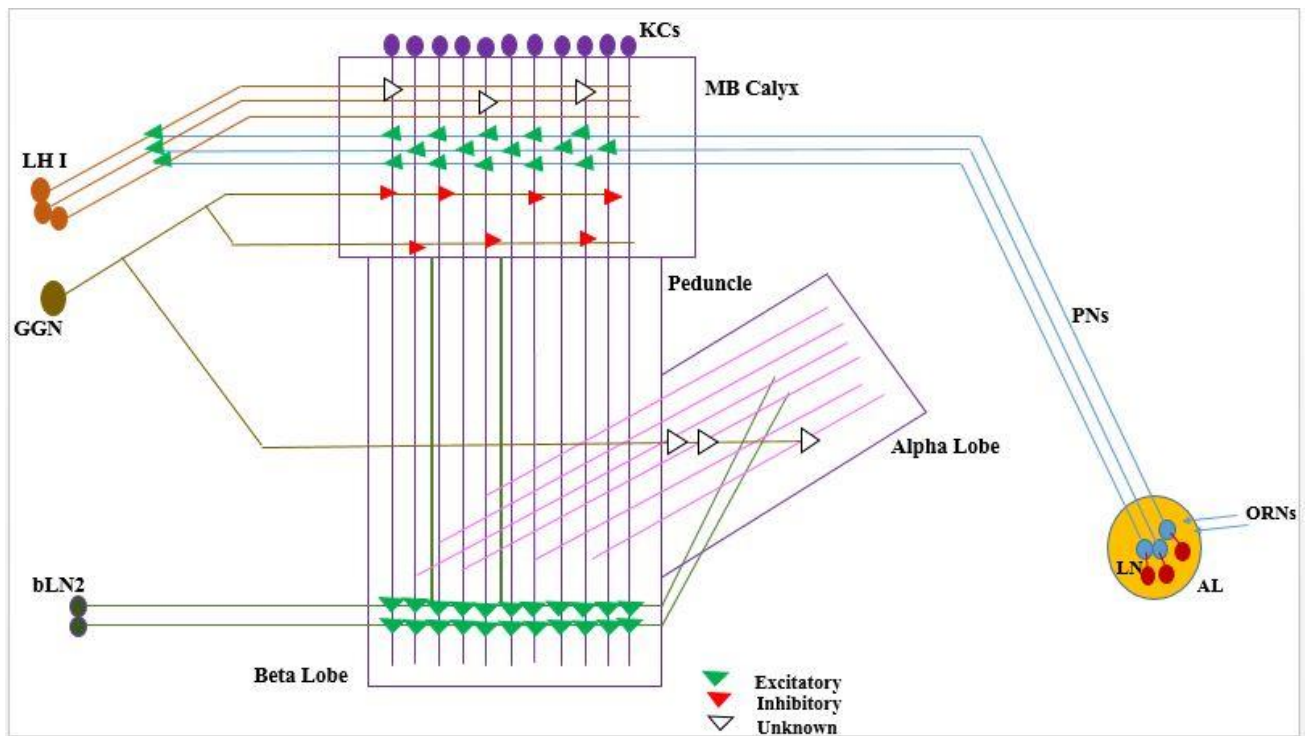


Fig 2. Schematic of Mushroom Body Network (Adapted from Laurent et al. 2007)

The objectives of this study were:

1. To construct a model of mushroom body network taking into account all feedback mechanisms known by incorporating connectivity, plasticities, physiology of each neuron type.
2. To predict the behavior and role of this circuit.
3. To understand how the mushroom body network is involved in olfactory associate memory

PROCEDURE

Based on literature survey and fills available of locust mushroom body, the morphology of the network was constructed in NEURON simulator using HOC programming.

Based on the distribution of channels, properties and its location in the Mushroom Body, each neuron was divided into sections while constructing the model.

In each neuron, the main sections included were soma, dendrite and axon.

HH (active conductances) were introduced in soma and axon sections and no HH (passive conductances) in dendritic sections.

The dimensions (Length and Diameter) of different sections used in our present model of Kenyon Cell and β Lobe Type II Neuron were based on the data collected from previous EM studies.

The following table gives the dimensions of different sections of KC and β LN2 neurons which we have used in our simulations:

	Diameter (μm)	Length (μm)	Location	Contains HH?
Soma	5	5	Periphery of calyx	Yes
Dendrite	0.5	100	Calyx region	No
Neurite	0.4	150	Calyx region	No
Axon	0.6	300	Peduncle	Yes
Axon branch in α Lobe	0.3	200	α Lobe	Yes
Axon branch in β Lobe	0.3	200	β Lobe	Yes

Table 3. Parameters used for the construction of KC morphology

(Laurent et al, 1993; Laurent, Leitch 1996)

MORPHOLOGY OF β LN2 MODEL:

	Diameter (μm)	Length (μm)	Location	Contains HH?
Soma	6	6	LPL	No
Dendrite	0.5	70	β Lobe	No
Neurite1	0.4	200	LPL	No
Neurite2	0.4	200	LPL	No
Axon1	2	200	Peduncle	Yes
Axon2	2	200	Peduncle	Yes

Table 4. Parameters used for the construction of β LN2 morphology

(Laurent et al, 1998)

Procedure followed during simulations:

Using NEURON:

We performed Current Clamp in our simulations. Each simulation lasted for 400 msec. After a delay of 100 msec from the start of simulation, current was injected for 100 msec (i.e. from 101 – 200 msec of the simulation) and the voltage responses were recorded from the time of current injection to the end of simulation. The values of positive currents injected ranged from 0 to 2.5 nA in increments of 0.05nA (except for the simulations of positive and negative feedback) and the values of negative currents injected ranged from 0 to -2.5 nA in steps of 0.05 nA. A Program was written in hoc to record the membrane potential and store them in a file. These files were further processed in MATLAB to plot the graphs.

MATLAB:

Calculation of Firing Frequency:

- Reading the data files which contained the membrane potential values from axon sections of KC and β LN2.
- Calculation of Sampling Rate (40000) based on dt value used in our simulations (0.025).
- Filtering the data between 300 and 1000 kHz using the function “butter” which can design a low pass filter.
- Using filtfilt function to apply the filter.
- Set a threshold value to determine all those data points greater than the threshold.
- Determine the location of peaks and their values in a simulation using the function “findpeaks”.
- Plot the data.
- Since each simulation lasted for 400msec and the delay was 100 msec, firing frequency was calculated using the formula: $[(\text{number of peaks}/300)*1000]$ spks/sec.
- For each value of current injected, firing frequency was calculated and the data stored as a .mat file.
- From this file, the plots were generated.

Single KC model:

We constructed a model of single KC with its various sections as indicated in the figure below. Positive current was injected into the dendrite (PNs synapse onto KC dendrites in the MB calyx) and the voltage traces in the soma, dendrite and axon sections of the KC were recorded with increasing value of currents and were compared. To span the parameter range of current values for which this particular cell continues to fire, we plotted spike rate in axon vs current injected.

To check for rebound, negative current was injected into the dendrite and the voltage traces recorded in the soma, dendrite and axon sections for different negative current values.

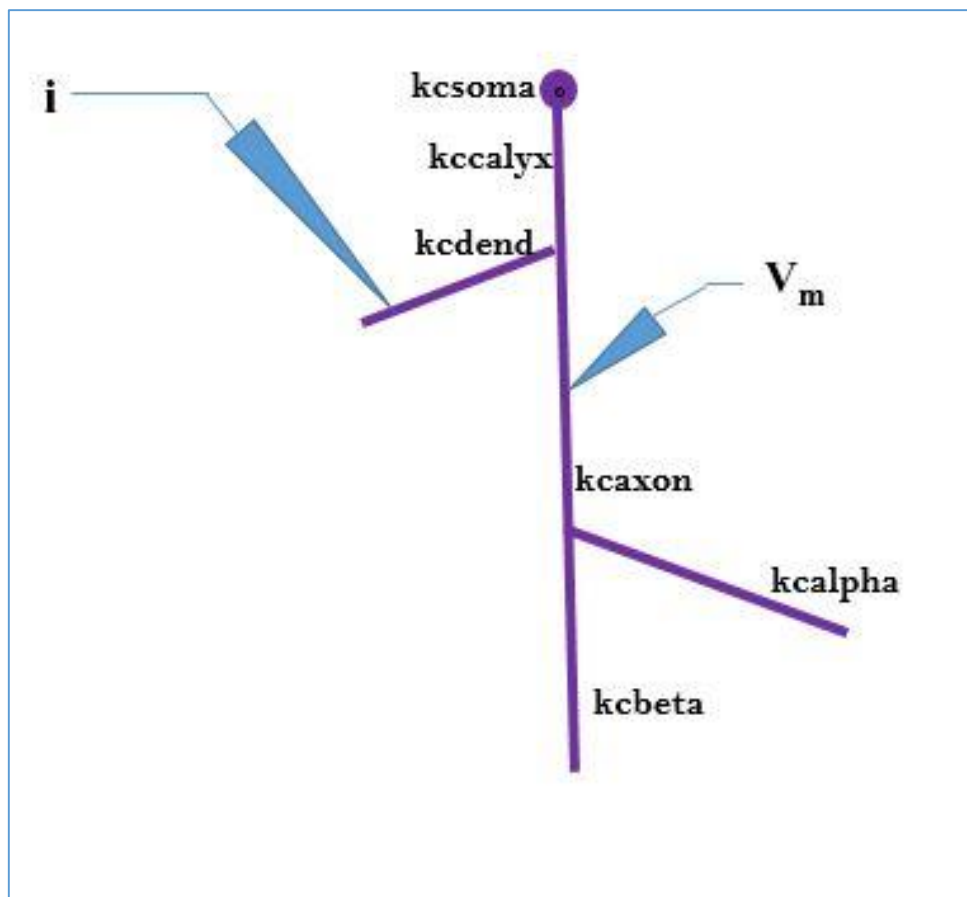


Fig 3. Schematic of single Kenyon Cell

Single β LN2 model:

We constructed a model of single β LN2 with its various sections as indicated in the figure below. Positive currents were injected into the β LN2 dendrite (β LN2 receives input from KC's through small neurites located in the β lobe of the mushroom body) and the membrane potentials in the soma, dendrite and axon sections were plotted and compared. To span the parameter range of current values for which this particular β LN2 model continues to fire, we plotted spike rate in β LN2 axon1 vs current injected. Similarly, to check for rebound, negative currents were injected into the dendrite and the voltage recorded and compared.

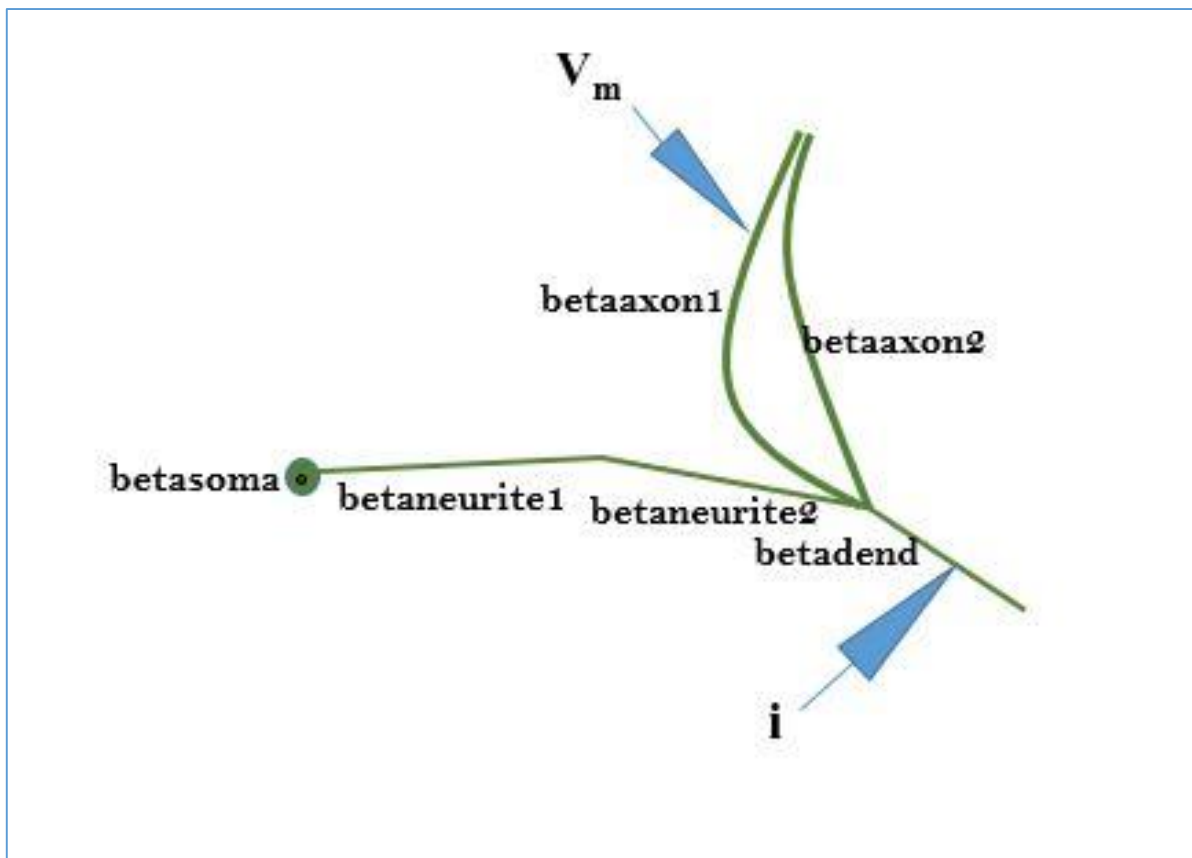


Fig 4. Schematic of single β LN2

Model of KC connected to β LN2:

We next connected the KC and β LN2 described previously with an excitatory synapse. The synapse was attached between the KC axon in β lobe and the dendrite of β LN2 in the β lobe. The weight of this synapse has been represented by $w1$. Current was injected into KC dendrite and the membrane potential was recorded from the axon and soma sections of β LN2. They were compared for increasing values of current injected and weight $w1$.

Change in spike rate in axon of β LN2 vs current injected was plotted for increasing value of weight ($w1$) of the synapse.

Spike rate in β LN2 was compared with spike rate in KC with increasing $w1$ values. It gives an estimate of parameter range for which spiking is observed.

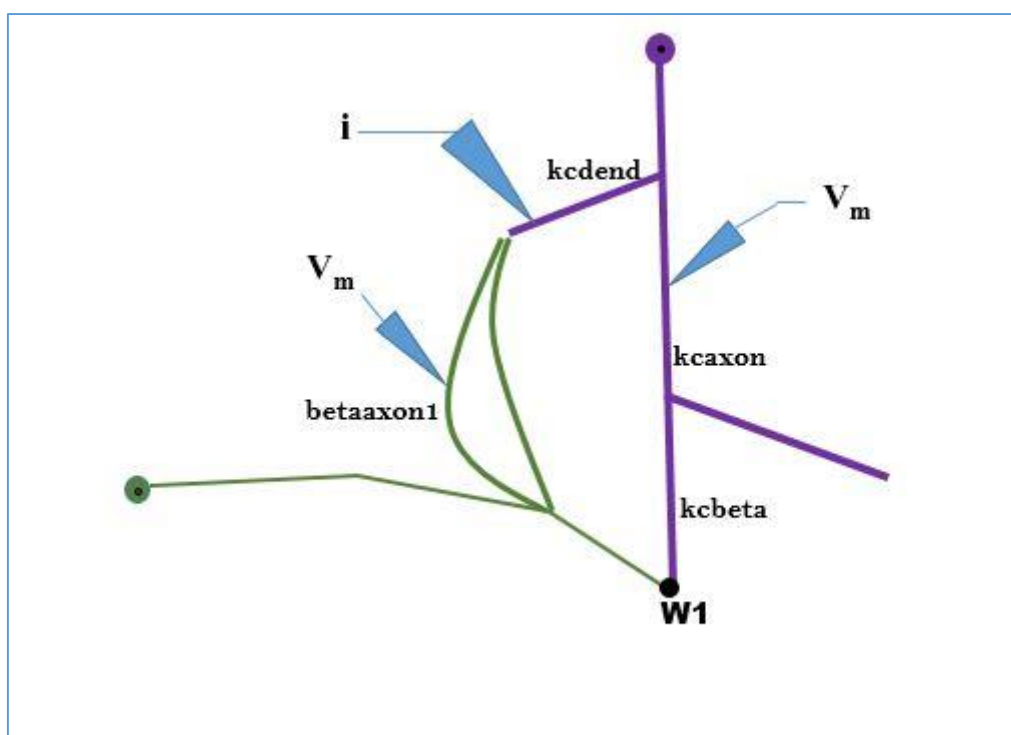


Fig 5. Schematic of KC connected to β LN2

Model of β LN2 connected to KC:

To understand the behaviour of the model without any feedback, we connected only β LN2 to KC.

From β LN2 to KC we connected an excitatory synapse as well as an inhibitory synapse. The weight of this synapse has been represented as w .

For both the synapses, we performed the following:

- We injected positive currents into β LN2 dendrite and recorded membrane potential from KC's soma and axon sections.
- For each section, we also compared the voltage for increasing weight w values.
- Similarly negative currents were injected, voltage was recorded and the data was plotted.

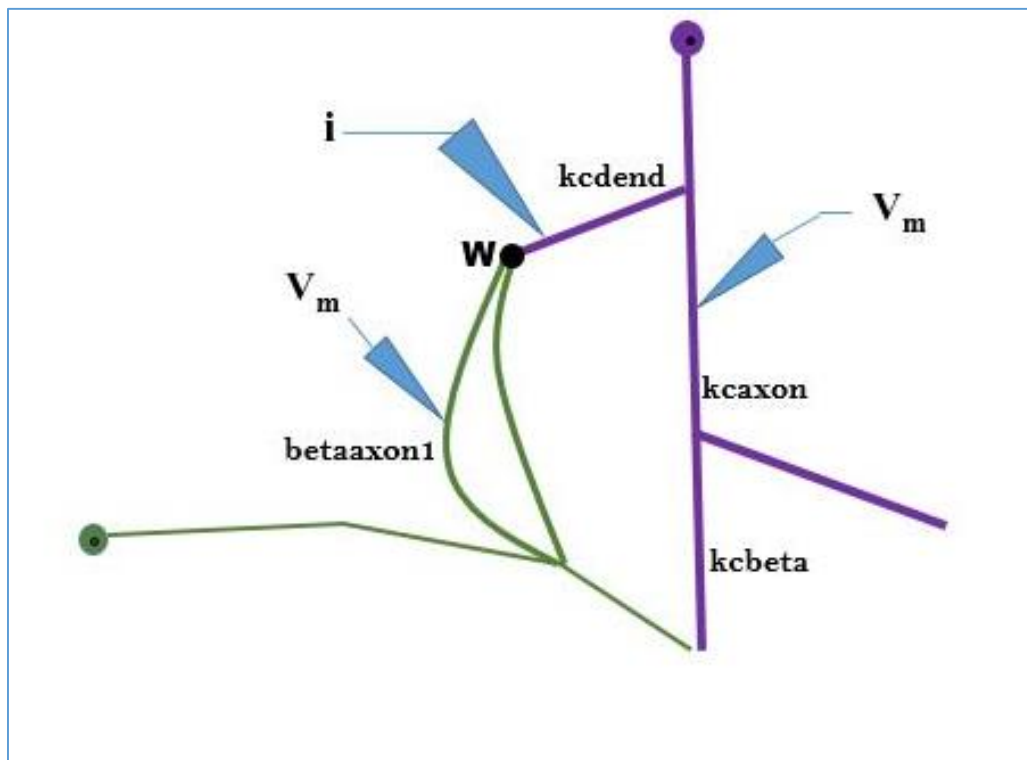


Fig 6. Schematic of β LN2 connected to KC

Model of β LN2 to KC Feedback:

To study the feedback from β LN2 to KC, we next connected both the synapses, one from KC to β (Excitatory; Weight is represented as w_1) and the other from β LN2 to KC (Weight is represented as w). We injected current (i) into KC dendrite and checked for the response in the axons of KC, β LN2 with different values of i , w_1 and w . The values of current injected ranged from 0 to 6 nA in increments of 1 nA. With the value of weight w_1 fixed, we plotted the spike rate vs current injected in these sections for increasing value of weight w .

Next to study how changing w_1 and w effects the spike rate, we compared the spike rate in β LN2 axon and KC axon with increasing values of w_1 and w in the case of positive feedback and also negative feedback. This was compared for two injected current values (3nA and 5nA). Thus we modelled both positive and negative feedback from β LN2 to KC.

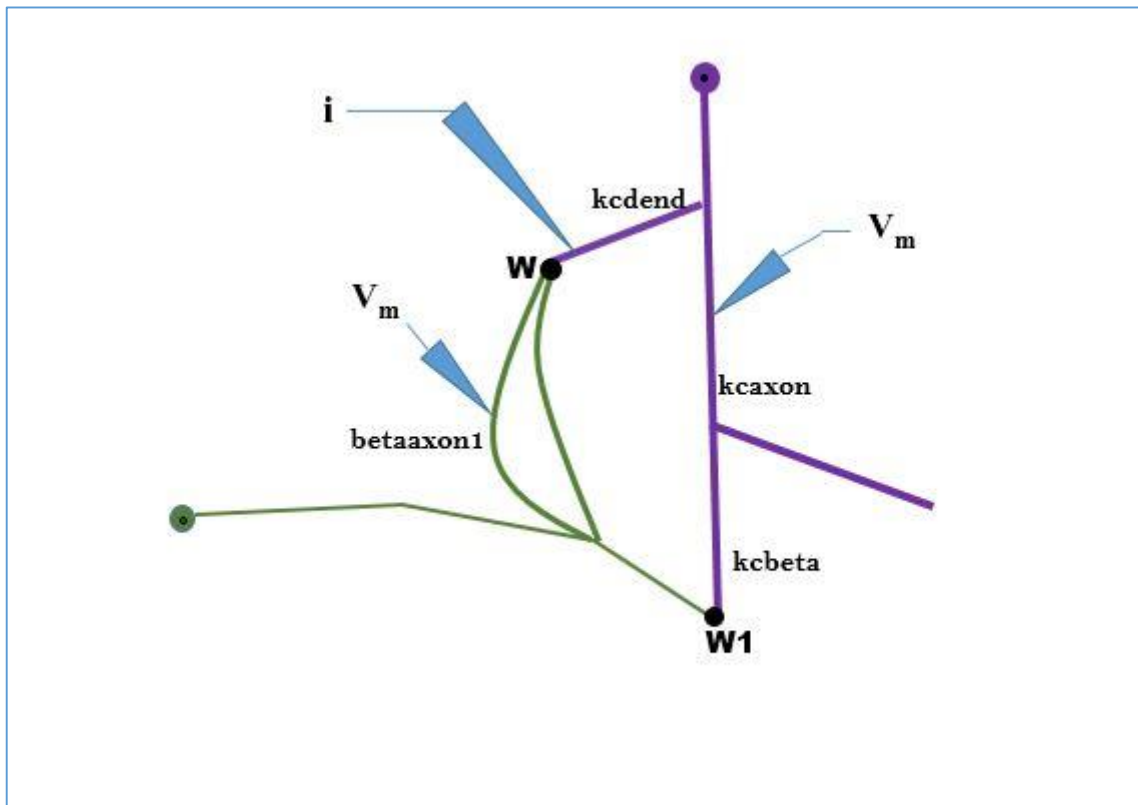


Fig 7. Schematic of KC - β LN2 feedback network

RESULTS AND DISCUSSION

1. Behaviour of a single KC towards positive currents:

The following graph is plotted between spike rate and current injected. It shows that the spike rate in KC axon increases with the increase in amount of current injected into KC dendrite.

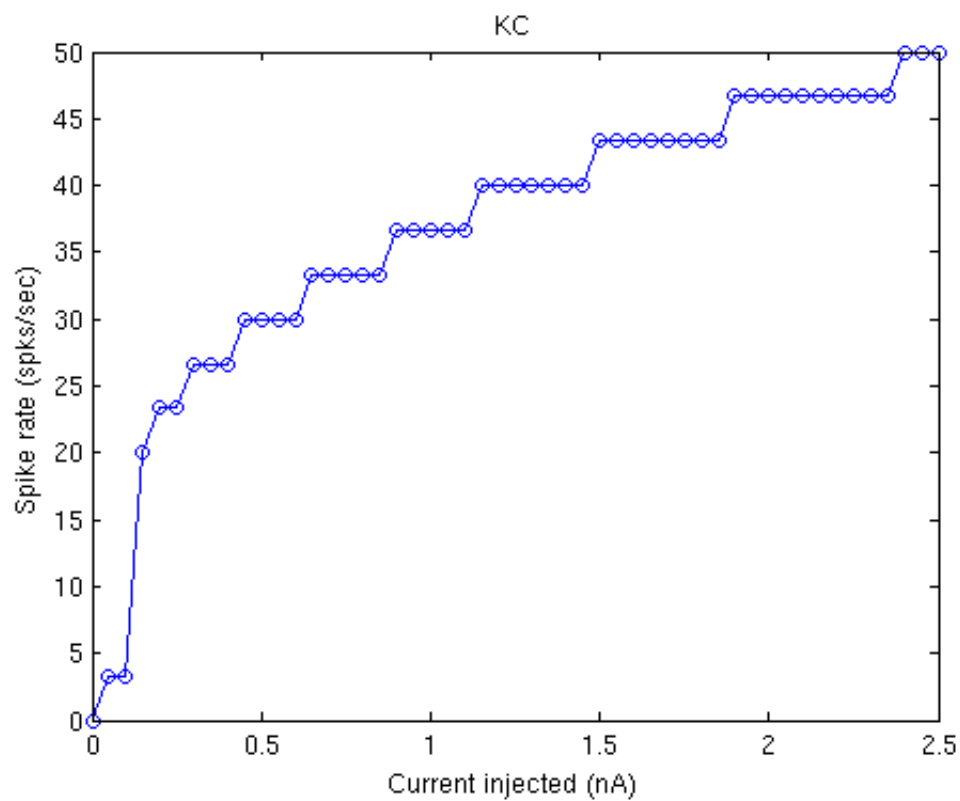


Fig 8. Spike Rate (spks/sec) in axon of Kenyon Cell with increasing value of positive currents ranging from 0 to 2.5 nA.

Traces of Membrane Potential at axon, soma and dendrite of KC:

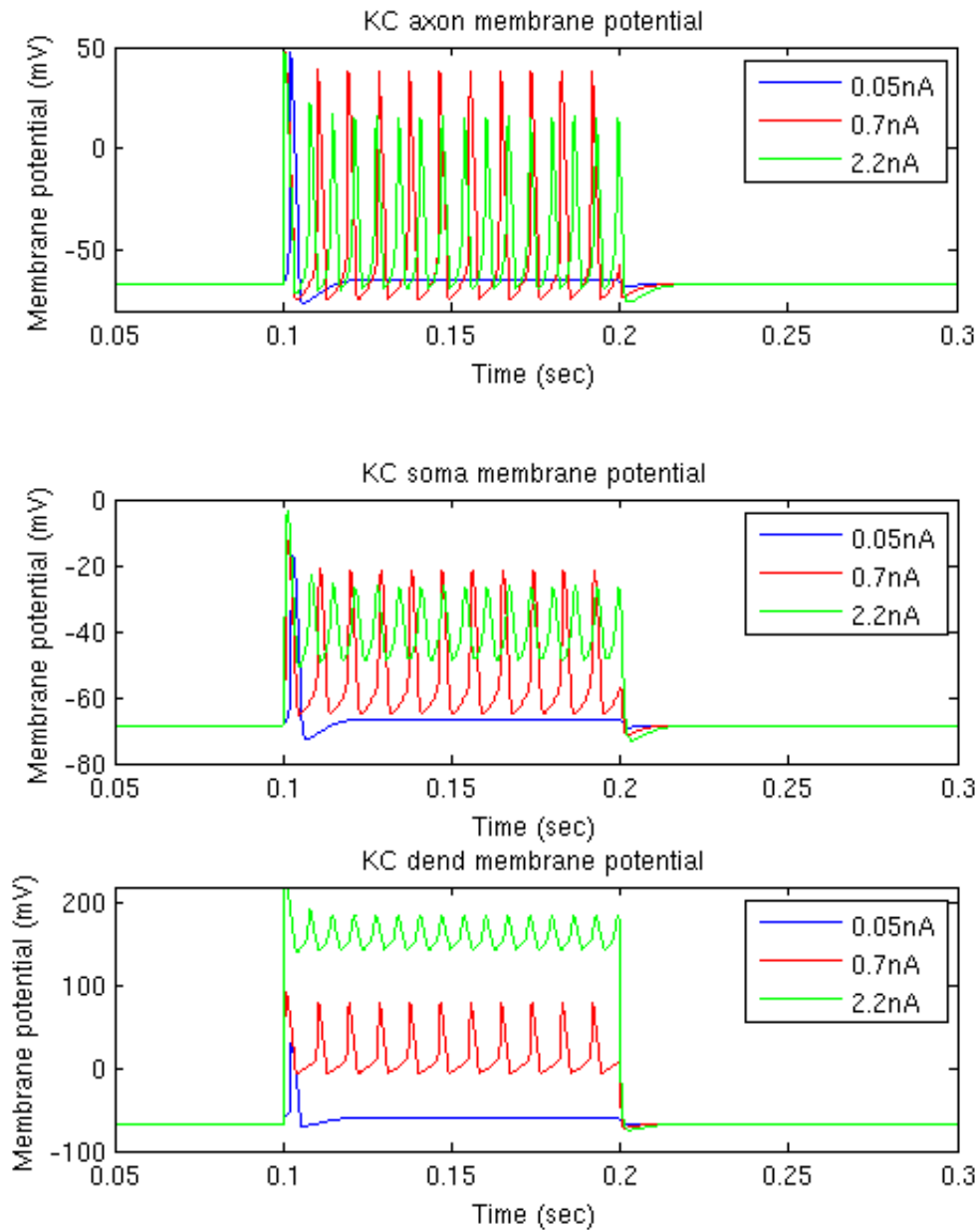


Fig 9. Membrane potentials in axon, soma and dendrite sections of KC for three values of current injected (0.05 nA, 0.7 nA, 2.2 nA). The blue graph corresponds to membrane potential in each section for 0.05 nA, the red graph for 0.7 nA and the green graph for 2.2 nA.

One spike can be seen for 0.05 nA of injected current and the spike count increases with the current injected in each section.

2. Behaviour of a single KC towards negative currents:

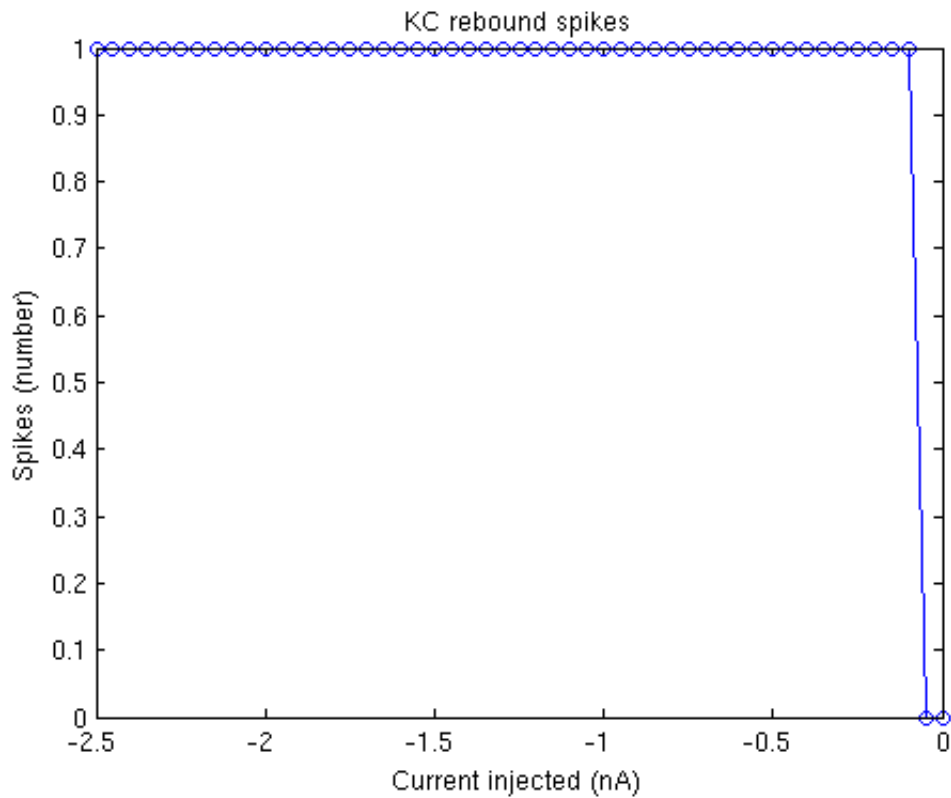


Fig 10. Rebound in KC axon with injected negative current into KC dendrite, with values ranging from 0 to - 2.5 nA.

With the present set of ion channels incorporated into the model, no matter how much the negative current injected into the KC dendrite is increased, there is always only one rebound seen. The number of rebounds rises sharply from 0 at 0 nA to 1 at 0.1 nA.

Traces of Membrane Potential at axon, soma and dendrite of KC:

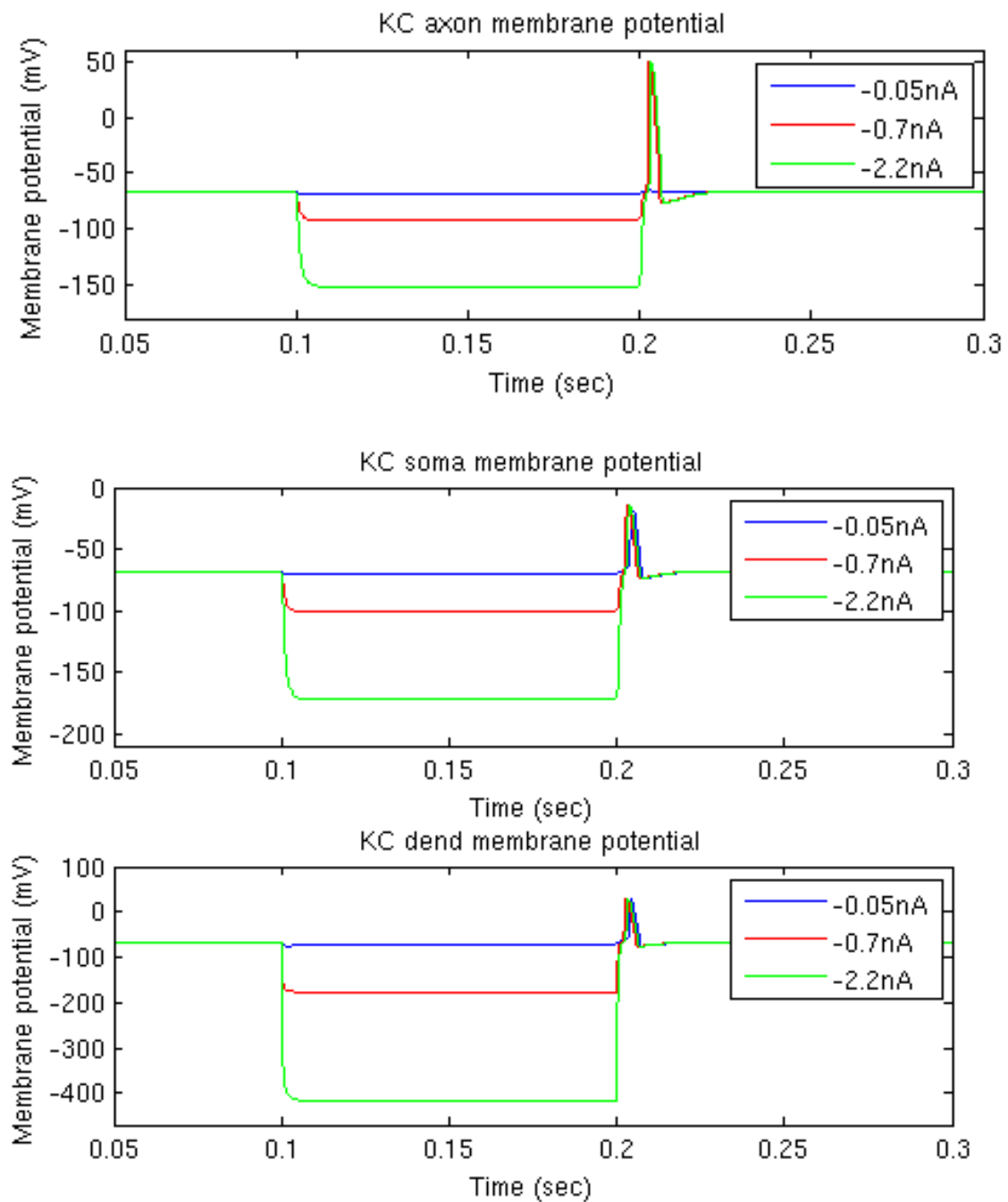


Fig 11. Membrane potentials in axon, soma and dendrite sections of KC for three values of current injected (-0.05 nA, -0.7 nA, -2.2 nA). The blue graph corresponds to membrane potential in each section for -0.05 nA, the red graph for -0.7 nA and the green graph for -2.2 nA.

Only one rebound is observed in all the sections and also at the same time with increasing negative currents.

3. Behaviour of a single β LN2 towards positive currents:

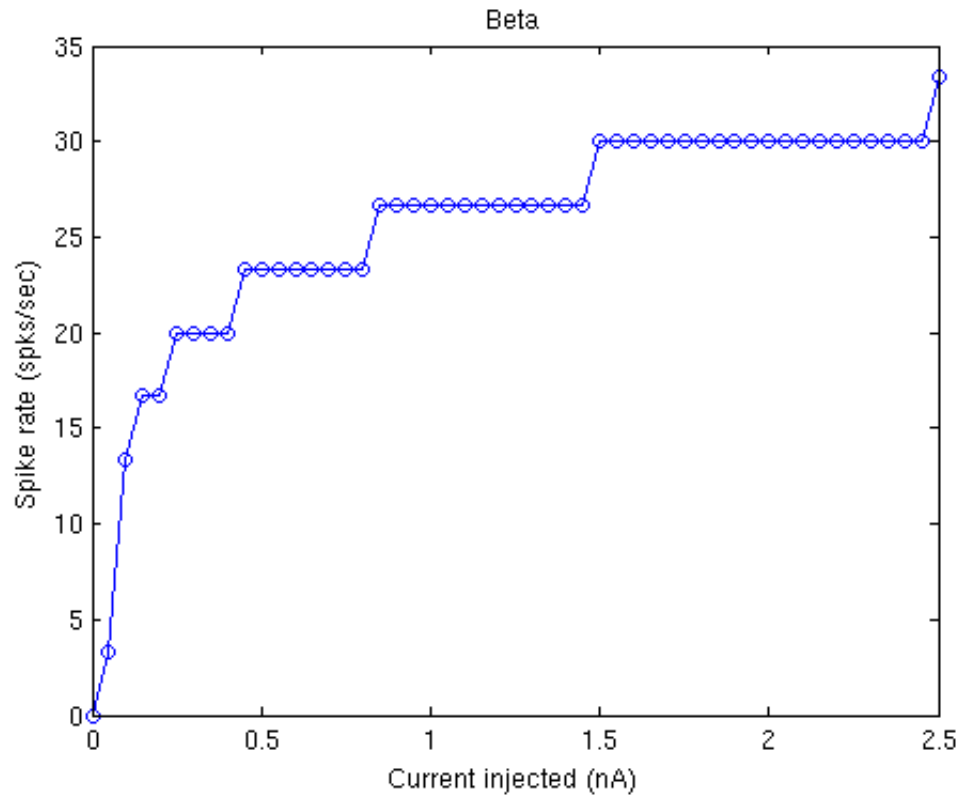


Fig 12. Spike rate (spks/sec) in axon of β LN2 neuron with increasing value of positive currents ranging from 0 to 2.5 nA.

Spike rate in axon of β LN2 neuron increases with the increase in amount of current injected into its dendrite.

Traces of Membrane Potential at axon, soma and dendrite of β LN2:

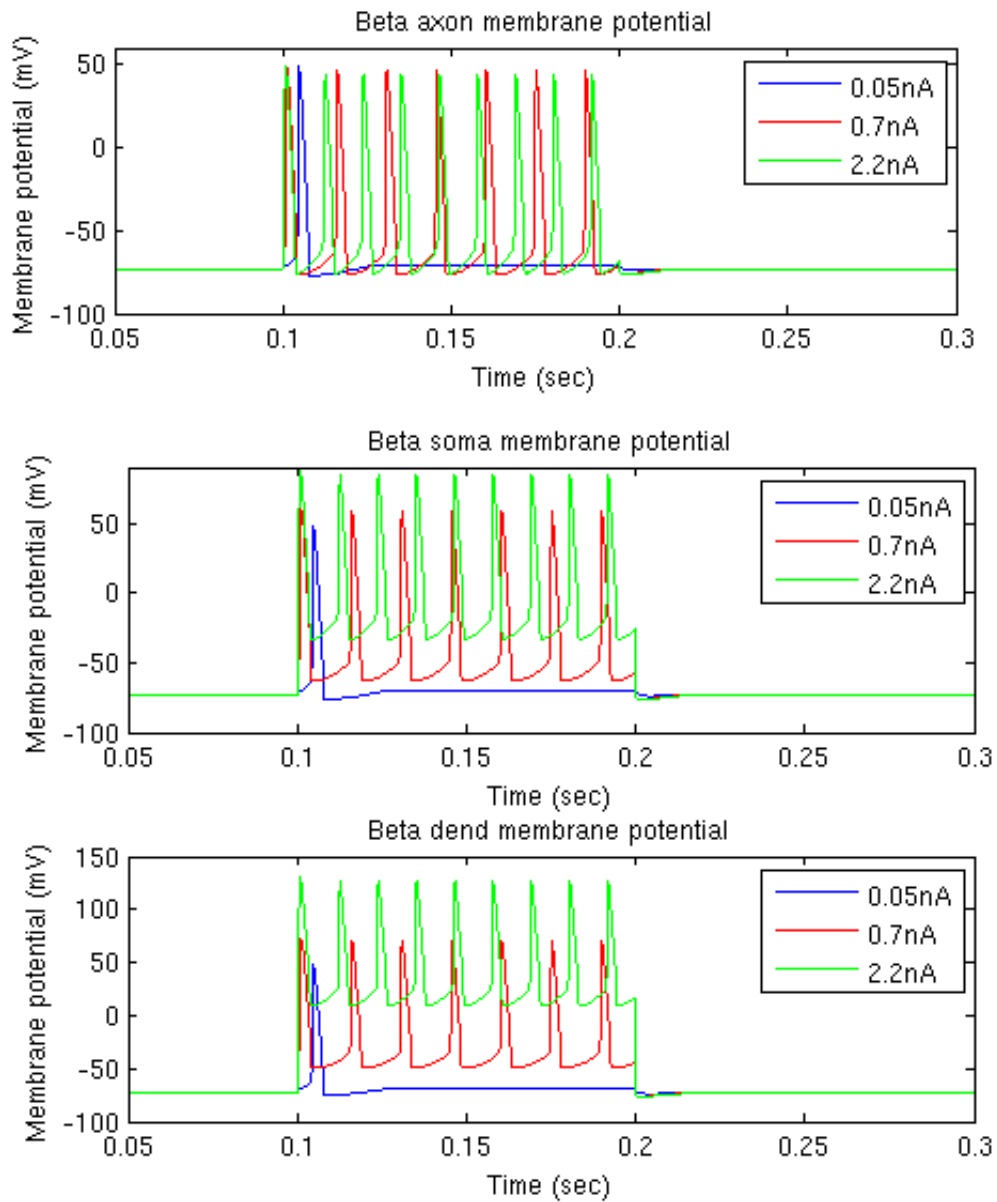


Fig 13. Membrane potentials in axon, soma and dendrite sections of β LN2 for three values of current injected (0.05 nA, 0.7 nA, 2.2 nA). The blue graph corresponds to membrane potential in each section for 0.05 nA, the red graph for 0.7 nA and the green graph for 2.2 nA.

One spike can be seen for 0.05 nA of injected current and the spike count increases with the current injected in each section.

4. Behaviour of a single β LN2 towards negative currents:

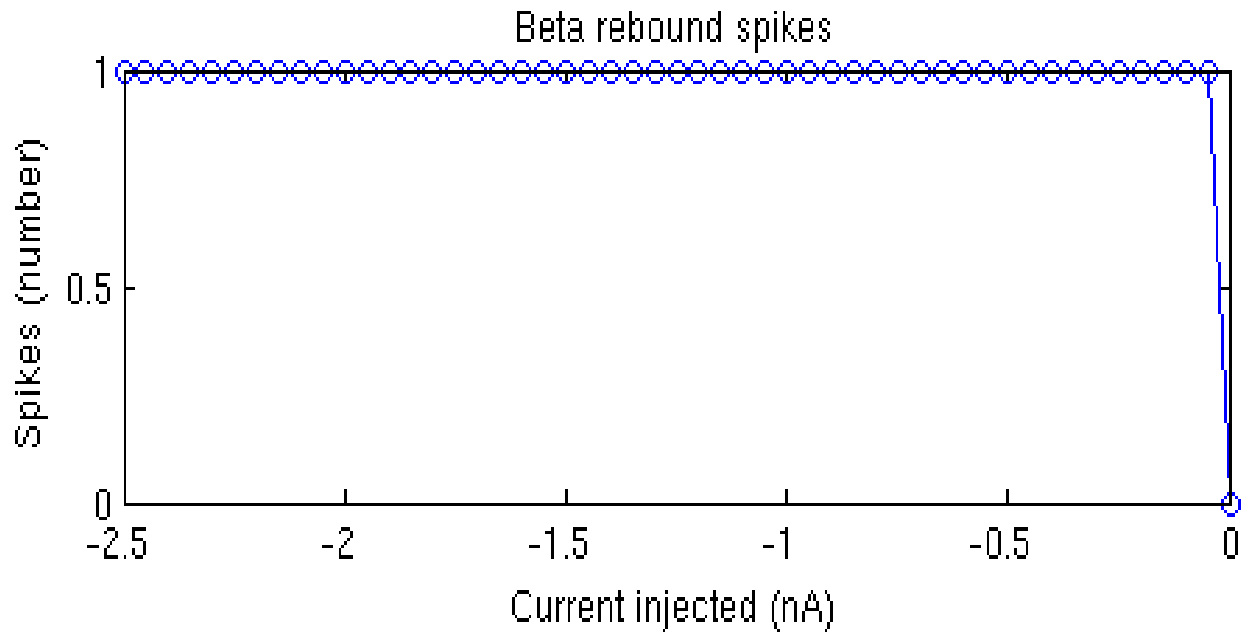


Fig 14. Rebound in β LN2 axon with injected negative current into β LN2 dendrite, with values ranging from 0 to -2.5 nA.

Similar to KC, no matter how much the negative current injected into β LN2 dendrite is increased, there is always only one rebound seen. The number of rebounds rises sharply from 0 at 0 nA to 1 at -0.1 nA.

Traces of Membrane Potential at axon, soma and dendrite of β LN2:

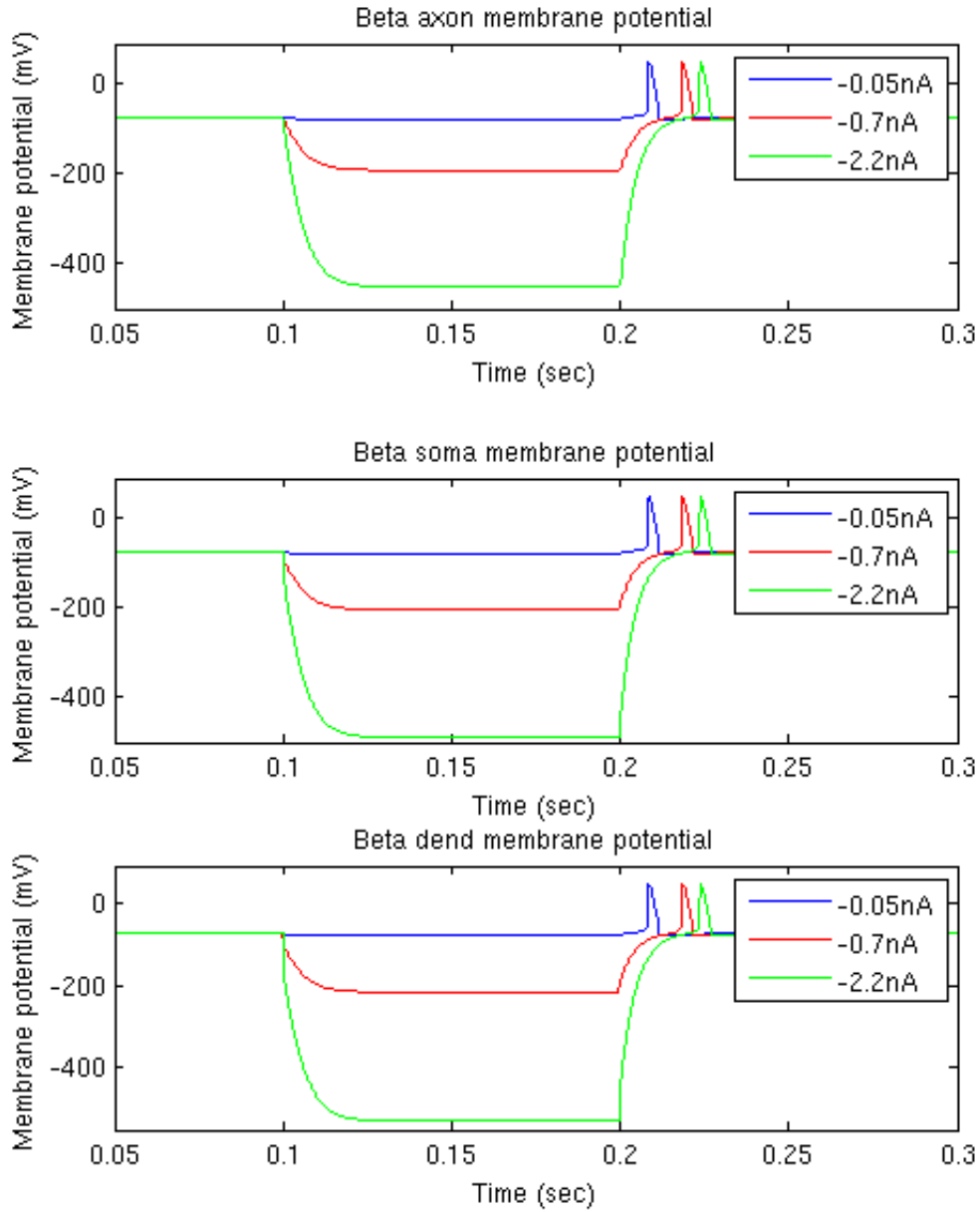


Fig 15. Membrane potentials in axon, soma and dendrite sections of β LN2 for three values of current injected (-0.05 nA, -0.7 nA, -2.2 nA). The blue graph corresponds to membrane potential in each section for -0.05 nA, the red graph for -0.7 nA and the green graph for -2.2 nA.

Only one rebound is observed in all the sections with increasing negative currents. However, in β LN2 there is a time lag observed between the rebounds for varying currents, which was not observed in KC.

5. With increasing currents injected into KC, β LN2 firing rate increases proportional to the synaptic weights:

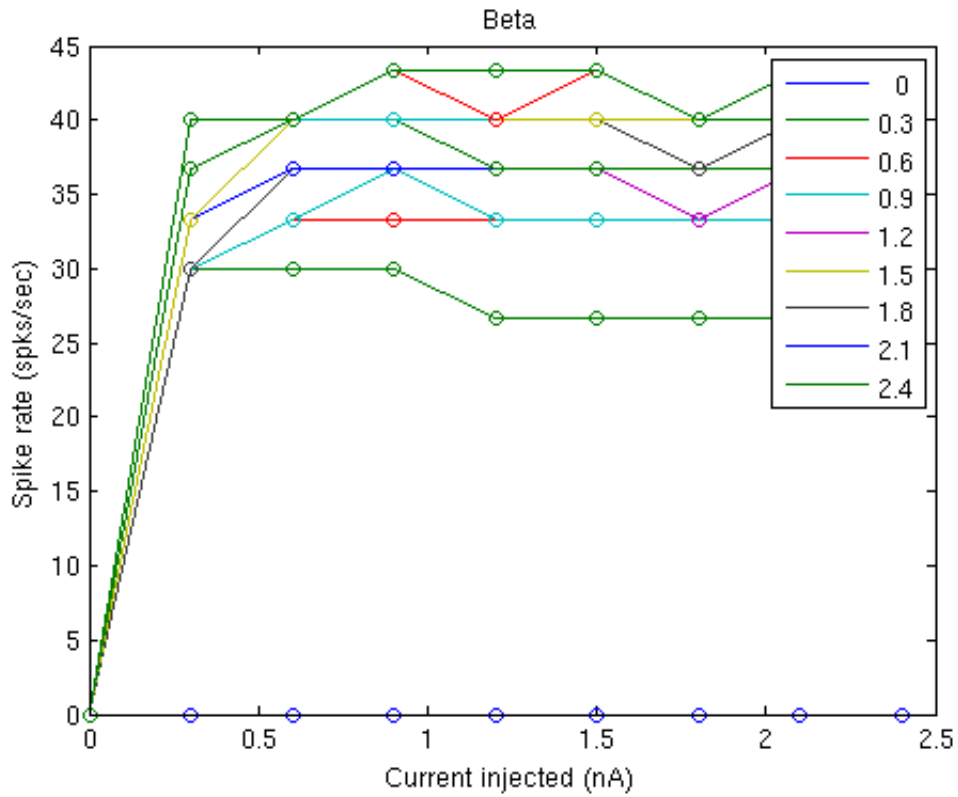


Fig 16. Spike rate (spks/sec) in β LN2 axon with increasing currents and increase in synaptic weights (w1).

The graph shows the spike rate in β LN2 axon at discrete points of finite intervals of current injected. The spike rate remains zero when weight is zero. When weight increases from 0 to 0.2, a sudden jump in the spike rate is observed. There exists a certain threshold value in the current injected and synaptic weights for which the spike rate increases dramatically and beyond the threshold not much change is observed. However, the graph could have been smoother if the duration of current injection was increased in our simulations.

Traces of Membrane Potential at soma of β LN2:

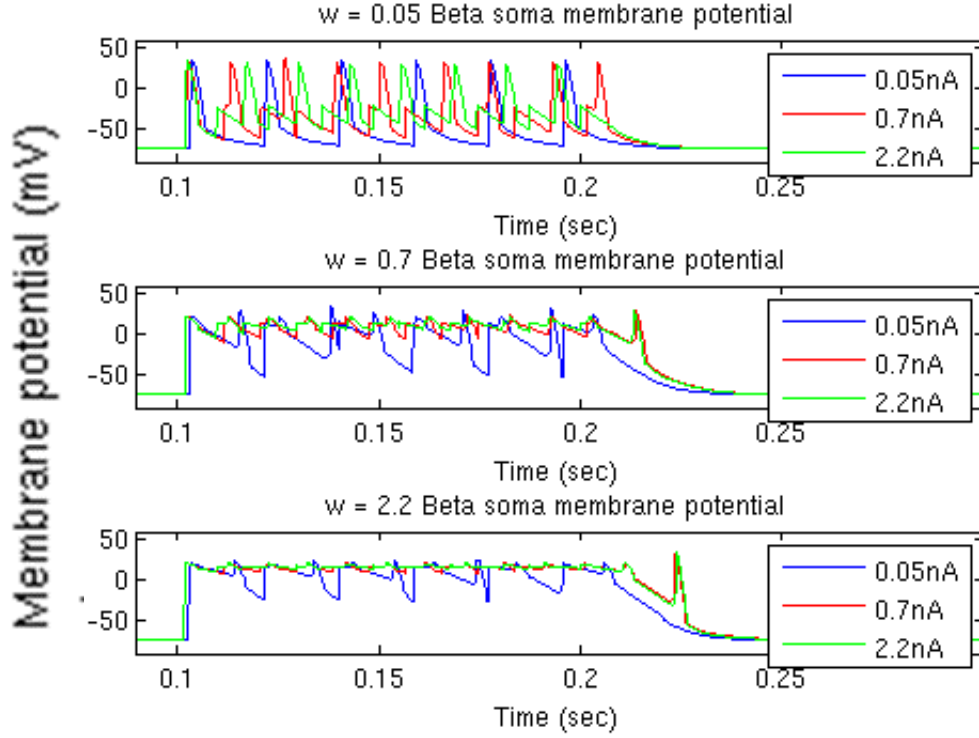


Fig 17. Membrane potentials in soma section of β LN2 for increasing values of synaptic weights ($w_1 = 0.05, 0.7, 2.2$) and current injected (0.05 nA, 0.7 nA, 2.2 nA) into KC dendrite. The blue graph corresponds to membrane potential in soma section for 0.05 nA, the red graph for 0.7 nA and the green graph for 2.2 nA.

At lesser weights, β LN2 soma's spike rate increases with increase in the current injected from 0 to 2.5 nA. However, this was not observed when the weights were increased further.

Traces of Membrane Potential at axon of β LN2:

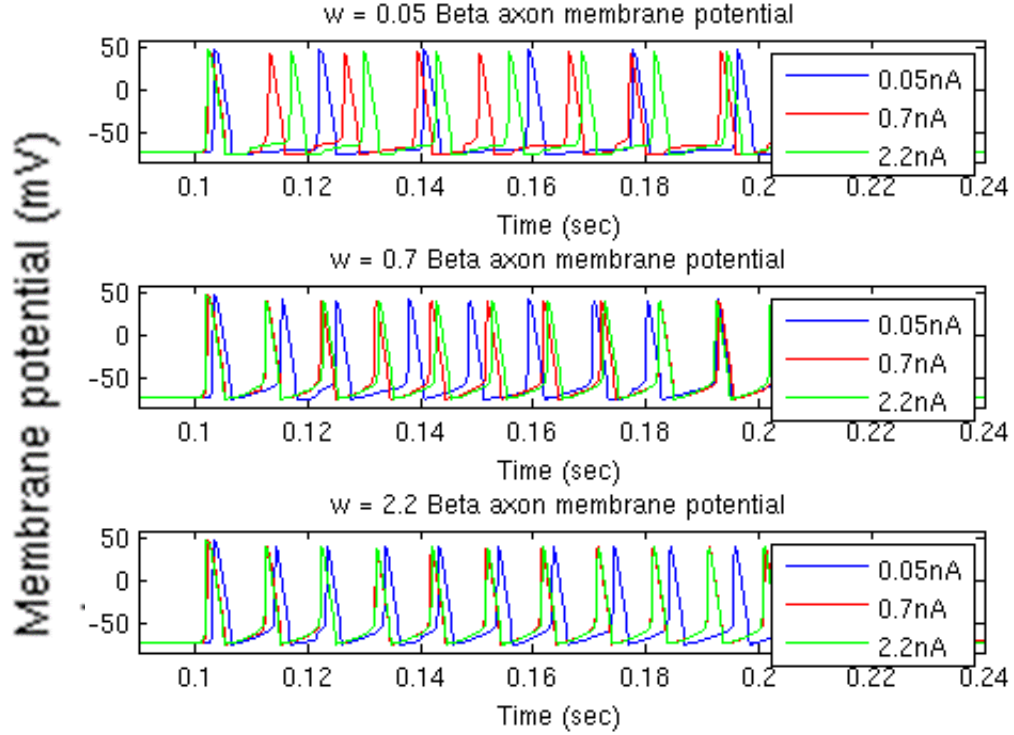


Fig 18. Membrane potentials in axon section of β LN2 for increasing values of synaptic weights ($w_1 = 0.05, 0.7, 2.2$) and current injected (0.05 nA, 0.7 nA, 2.2 nA) into KC dendrite. The blue graph corresponds to membrane potential in axon section for 0.05 nA, the red graph for 0.7 nA and the green graph for 2.2 nA.

For a particular value of current injected, the spike rate in β LN2 axon increased with increase in synaptic weight w . Here w_1 corresponds to the synapse from KC to β . (In which KC is the presynaptic neuron and β is the post synaptic neuron).

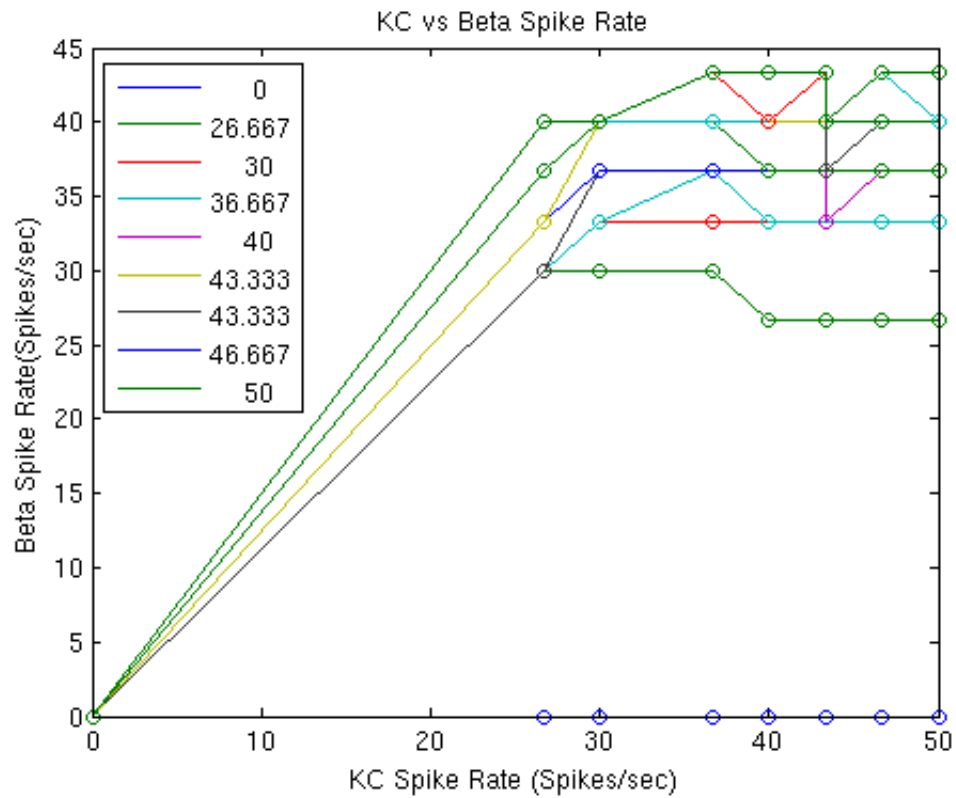


Fig 19. β LN2 spike rate vs KC spike rate with increasing w_1

KC has a very steep firing rate. These being uniform currents, up to a certain value of current injected, it doesn't spike and later changes dramatically.

6. Excitatory synapse between β LN2 and KC :

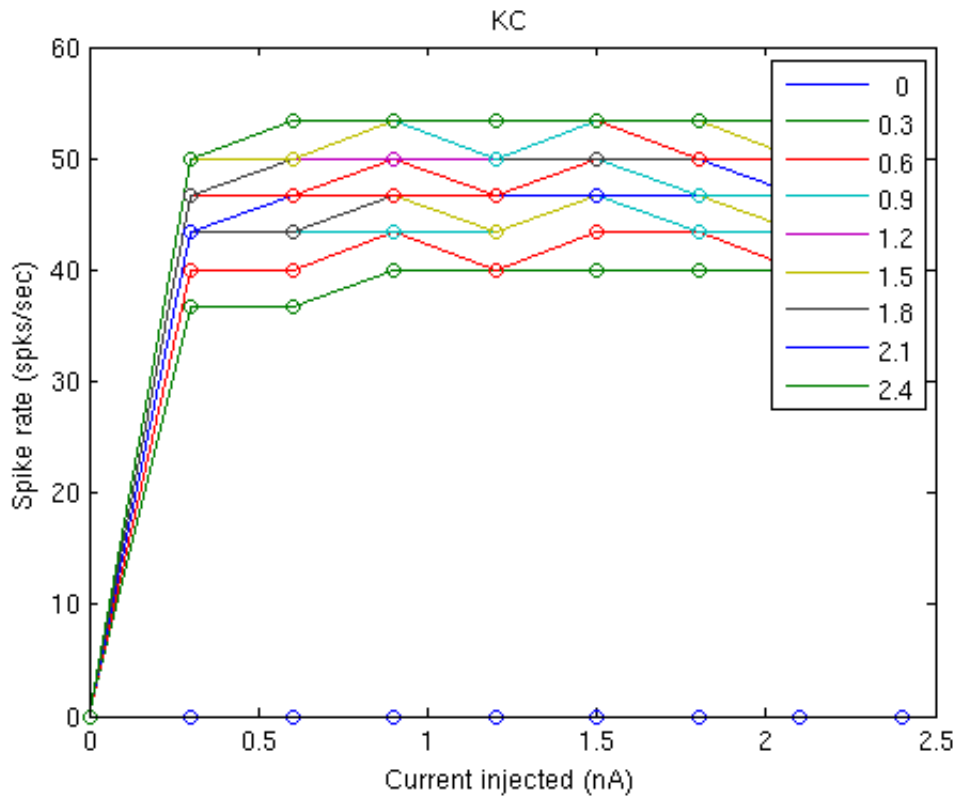


Fig 20. Spike rate (spks/sec) in KC axon with increasing currents and increase in synaptic weights (w).

The spike rate remains zero when weight w is zero. When w increases from 0 to 0.3, a sudden jump in the spike rate is observed. Spike rate increases with a certain threshold value.

Spike rate increases with currents and is proportional to synaptic weights

Traces of Membrane Potential at soma and axon of KC:

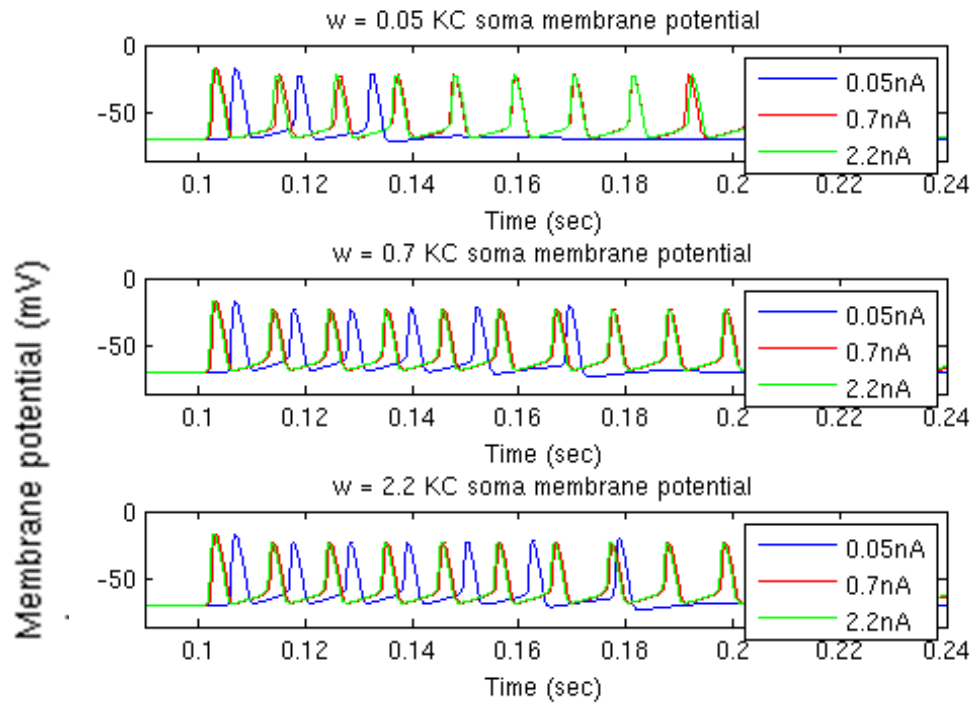


Fig 21. Membrane potentials in KCsoma for increasing values of i and w

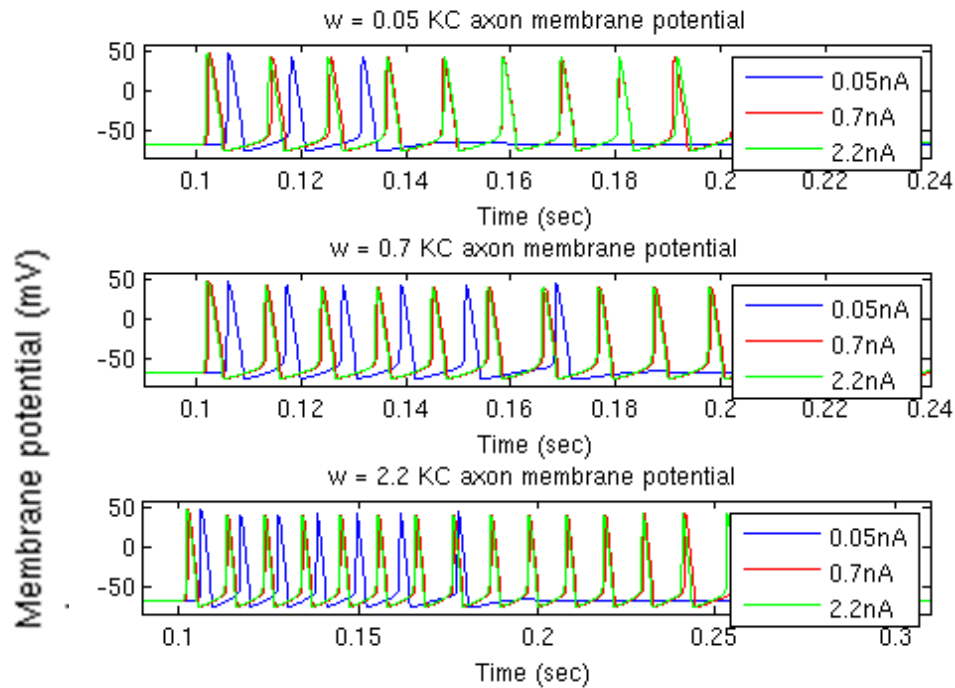


Fig 22. Membrane potentials in KC axon for increasing values of i and w

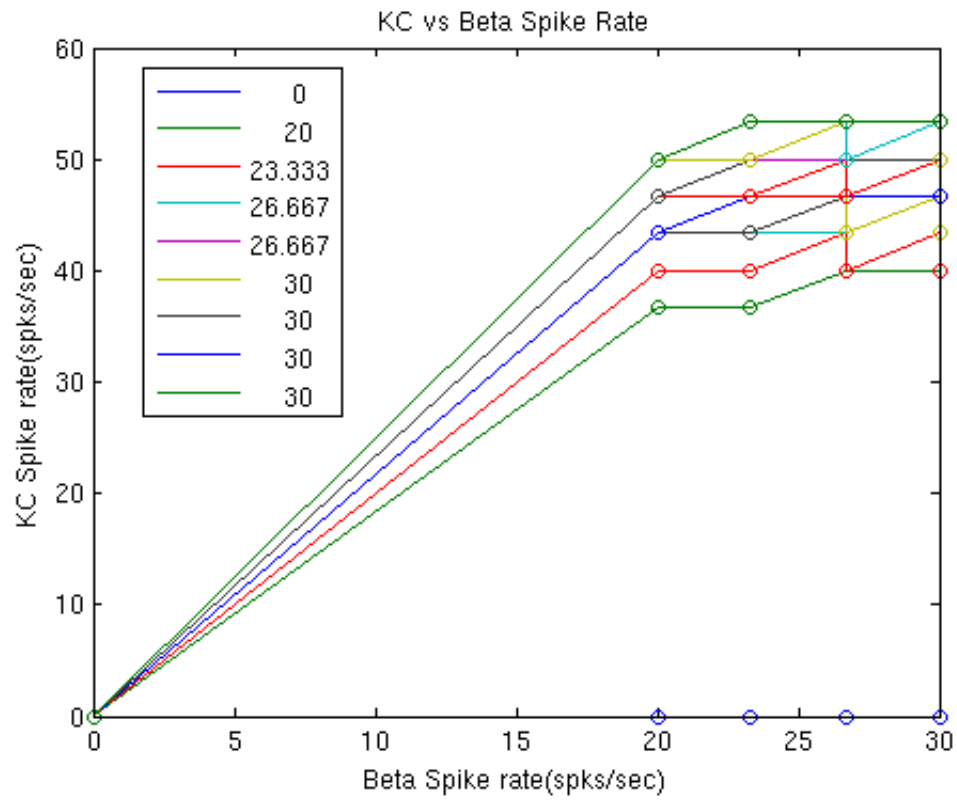


Fig 23. KC spike rate vs β LN2 spike rate with increasing w

β LN2 has a very steep firing rate. These being uniform currents, up to a certain value of current injected, it doesn't spike and later changes dramatically.

7. Inhibitory current from β LN2 to KC:

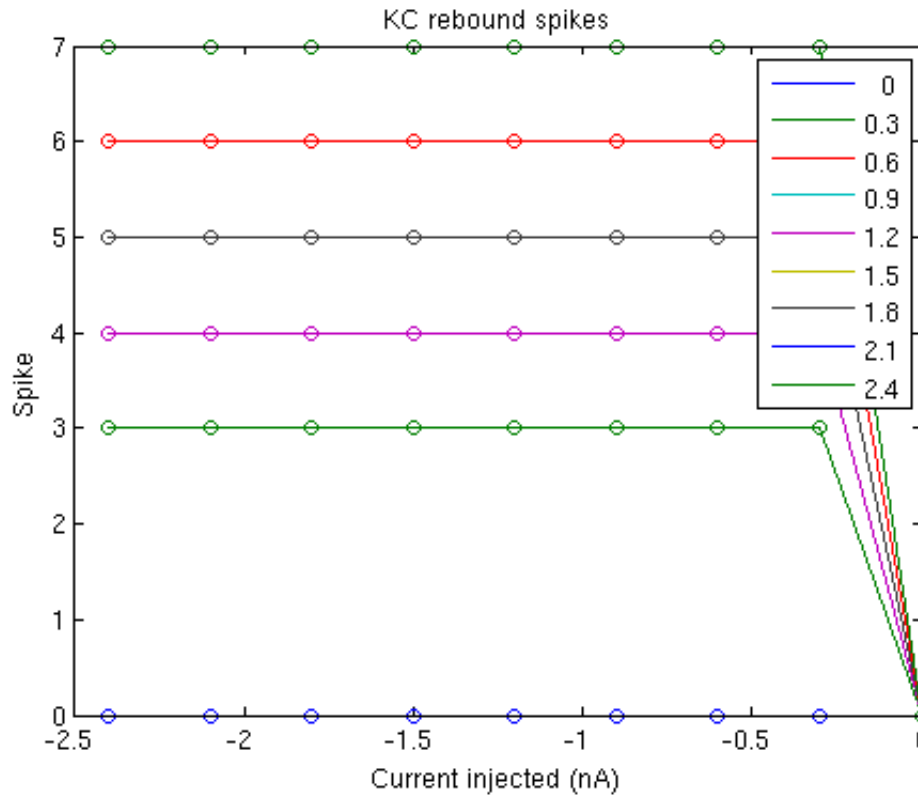


Fig 24. Rebound in KC axon with injected negative current into β LN2 dendrite.

With increase in current injected, the number of spikes remain the same for any given weight. The number of spikes increases with increase in weight w .

8. Inhibitory synapse between β LN2 and KC works as expected:

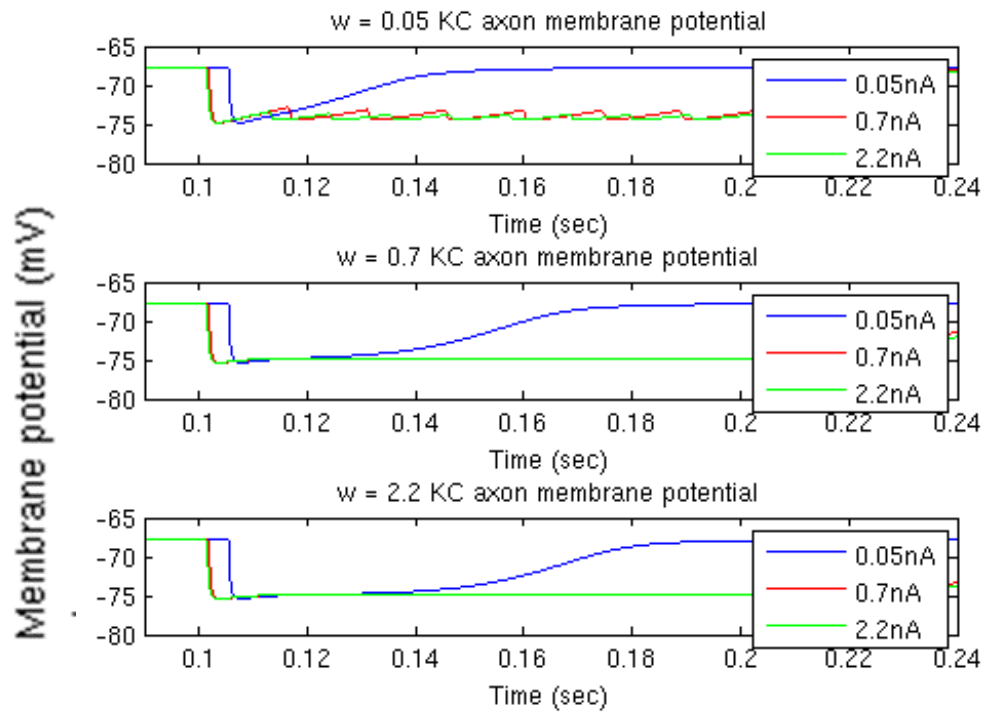


Fig 25. Membrane potentials in KC axon for increasing values of i and w

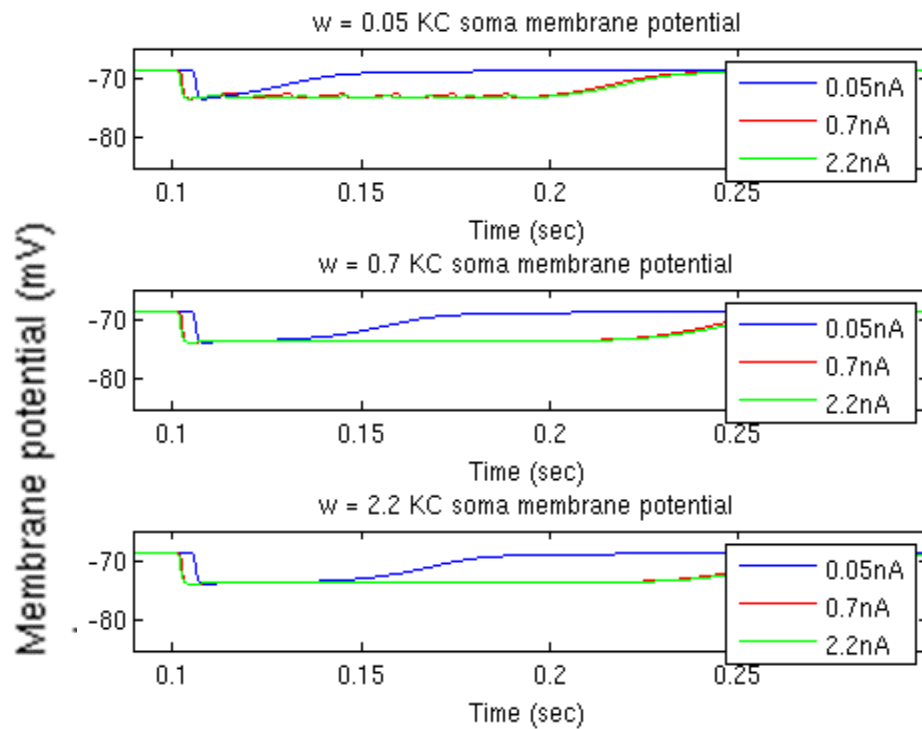


Fig 26. Membrane potentials in KC soma for increasing values of i and w

9. β LN2 \rightarrow KC : Inhibitory synapse negative currents

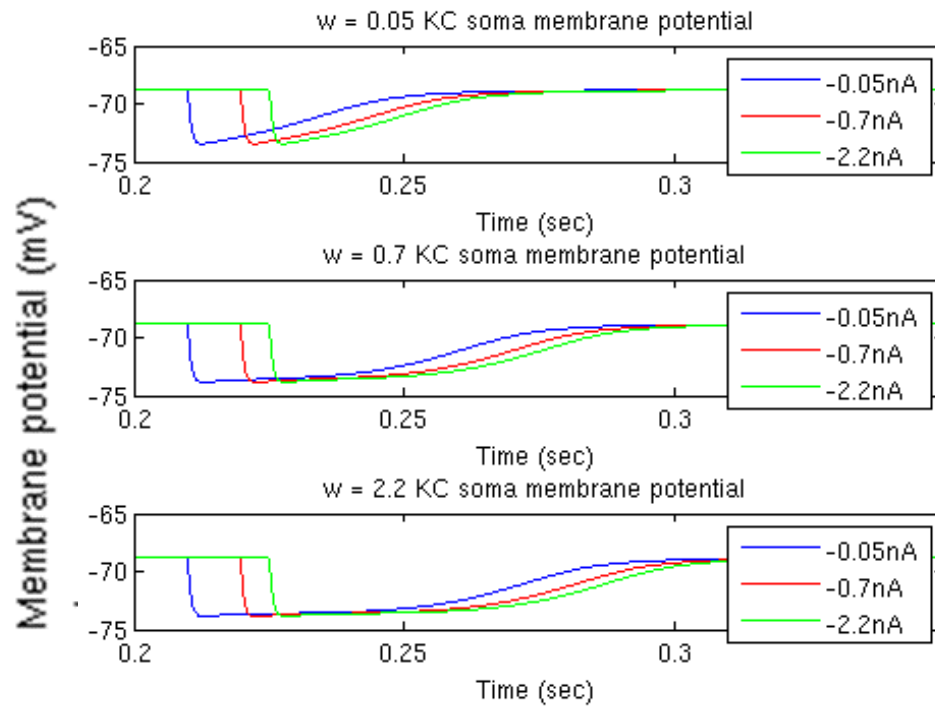


Fig 27. Membrane potentials in KC soma for different negative currents and weight w .

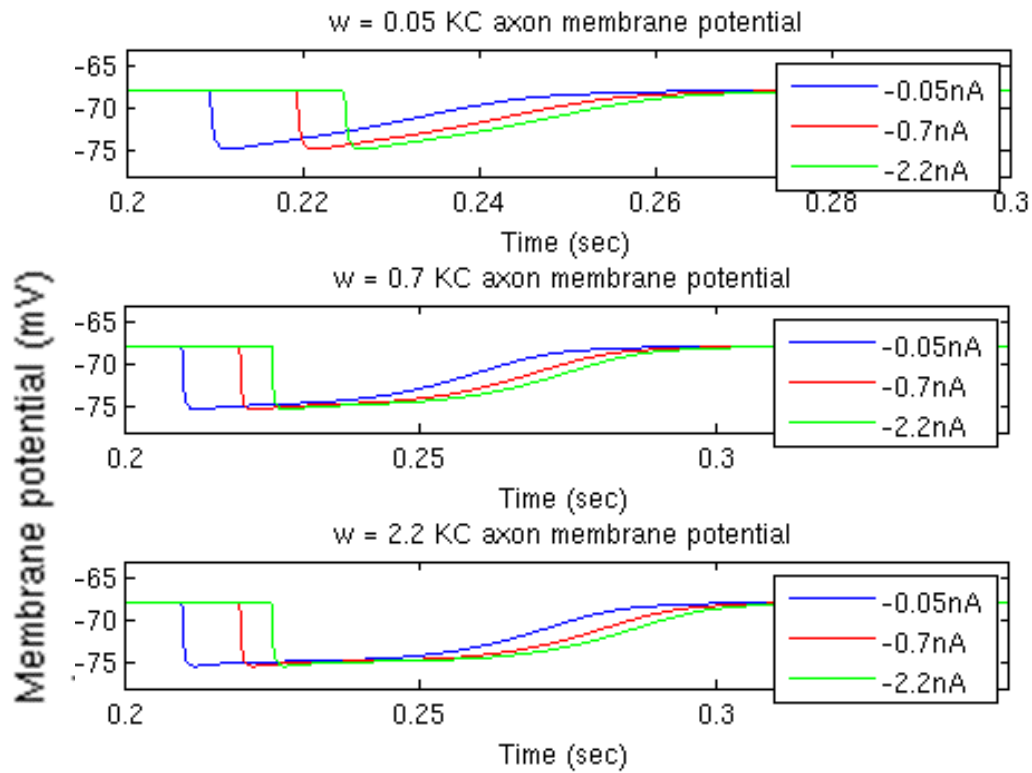


Fig 28. Membrane potentials in KC axon for different negative currents and weight w .

10. Behaviour of KC and β LN2 with positive and negative feedback:

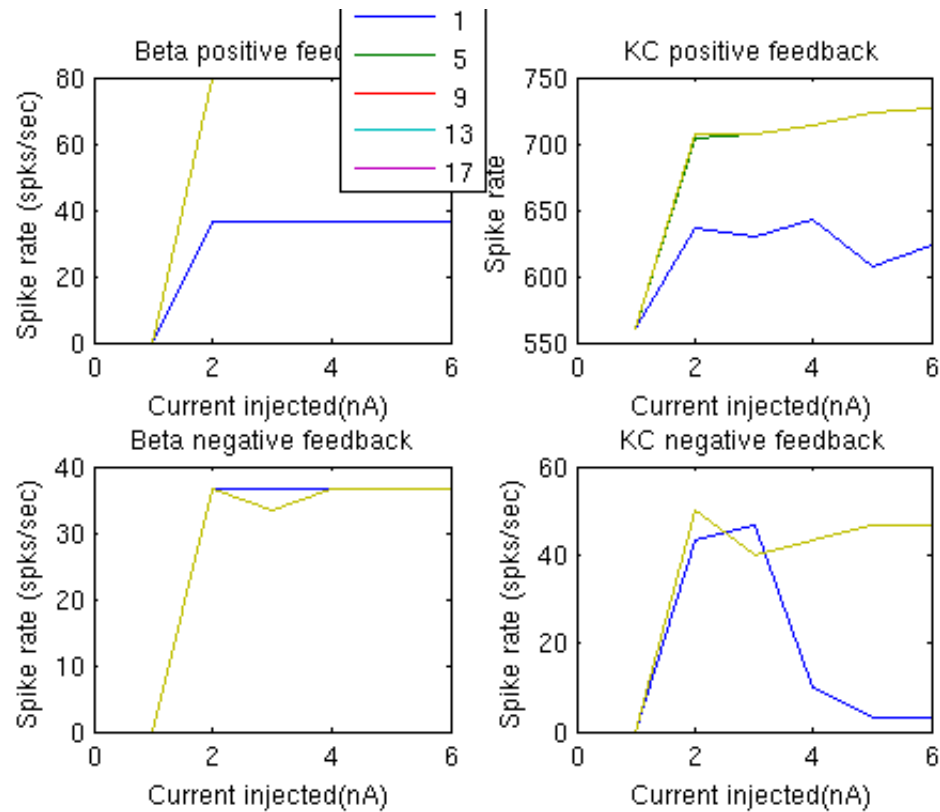


Fig 29. Comparison of spike rate during positive and negative feedback for a fixed w_1 and increasing w values. These correspond to axon sections of KC and β LN2 as indicated.

In positive feedback, spike rate increases with increase in w values.

However, in negative feedback, the spike rate, though initially decreases, later increases with increase in injected current. This is in contrast to what was expected.

11. Effect of changing w_1 and w weights on spike rate:

Below are figures explaining the change in spike rate in KC and β LN2 axon in positive and negative feedback for two different increasing current values.

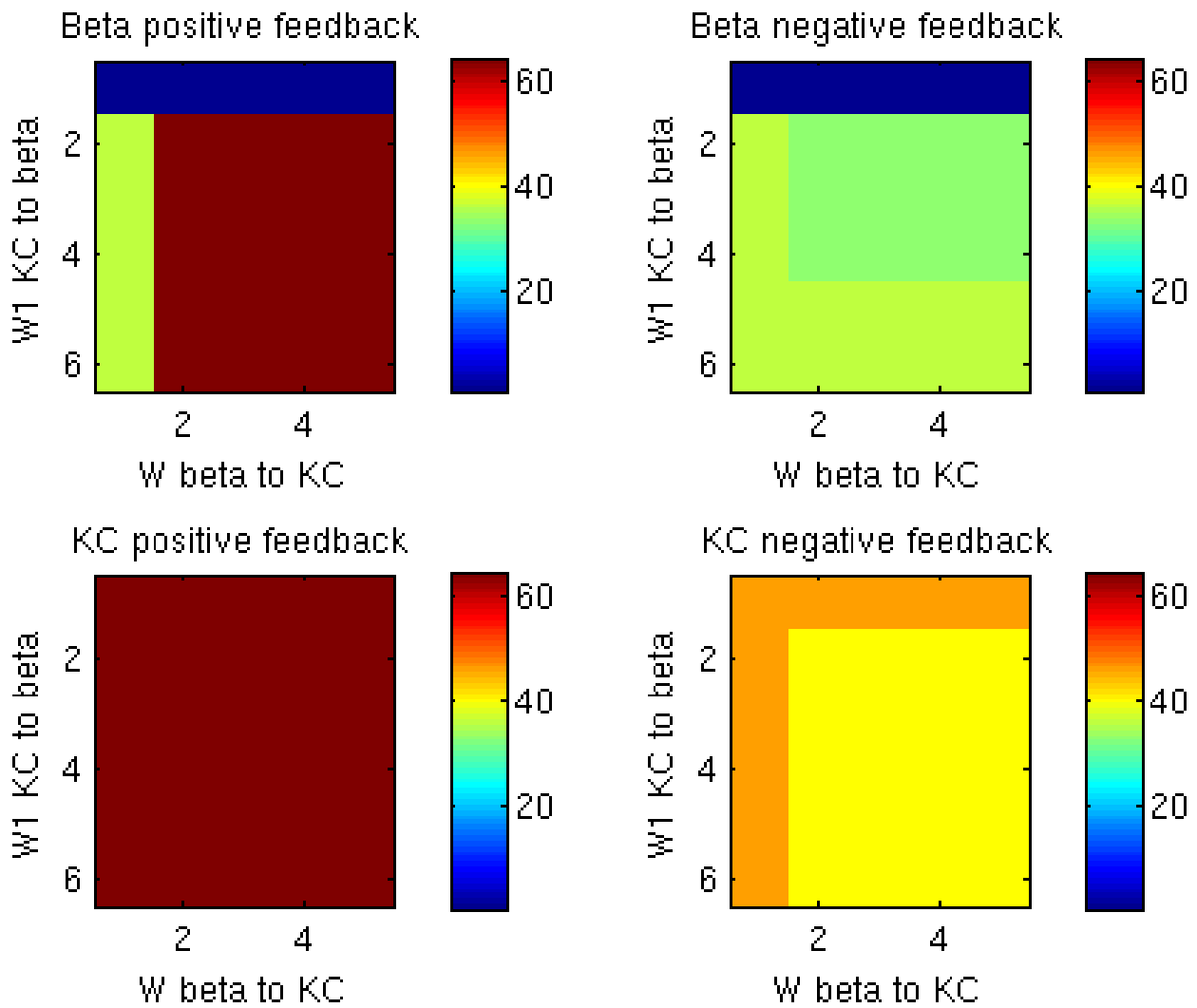


Fig 30. Spike rate in positive and negative Feedback when $i = 3nA$. Color bar represents spike rate.

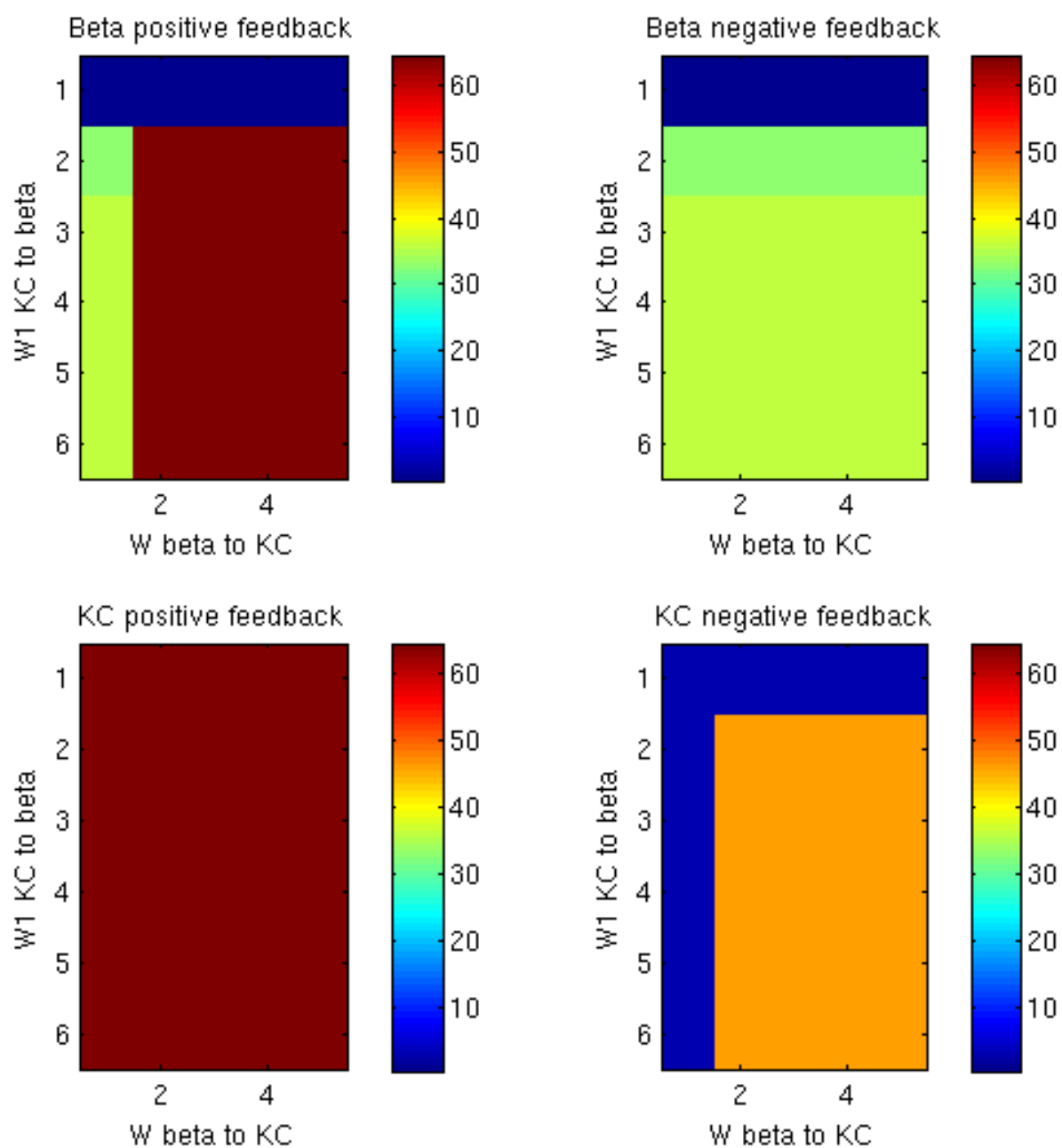


Fig 31. Spike rate in positive and negative feedback when $i = 5\text{nA}$. Color bar represents spike rate.

For the particular combination of w_1 , w values used, we observed the following:

- In positive feedback, the spike rate saturated in both KC and β LN2 when we increased the current injected.
- Negative feedback seemed to be obeyed only for a particular value of injected current (3nA).
- The spike rate increased when we increased the current injected during Negative Feedback to 5nA.

CONCLUSIONS

- We were able to construct the KC and β LN2 models with only Voltage gated Na and K channels (i.e. with HH alone).
- These models show an increase in firing rate with increase in current injected.
- The KC and β LN2 models, without any other channels incorporated except HH, will not have more than one spike no matter how much ever the negative current injected is increased.
- We attempted to study the change in firing rate in positive and negative feedback from β LN2 to KC.
- In positive feedback, we could not find a combination of w , w_1 that would cause the recurrent excitation to die out on its own.
- With the range of weights chosen in our particular model, in the negative feedback, firing rate goes down in a certain regime of current injected.

FUTURE DIRECTIONS

The next course of action in trying to understand this feedback would be:

- To incorporate STDP in the synapse from KC to β LN2.
- To incorporate post-synaptic inhibitory and excitatory type of β LN2.
- To model other ion channels and incorporate them in our model using NMODL.
- To increase the number of KC's and β LN2's in our model and perform simulations.
- To perform simulations for stochastic excitation of KC's.

REFERENCES

1. **Sabine Schafer, Hendrik Rosenboom, and Randolph Menzel.** (1994). Ionic currents of Kenyon cells from the mushroom body of the honeybee. *J.Neurosci.* 14(8):4600-12.
2. **Leitch B, Laurent G.** (1996). GABAergic synapses in the antennal lobe and mushroom body of the locust olfactory system. *J.Comp.Neurol.* 2; 372(4):487-514.
3. **Gupta and Stopfer.** (2014). A Temporal Channel for Information in Sparse Sensory Coding. *Current Biology* 24, 1-10.
4. **Katrina MacLeod, Alex Backer & Gilles Laurent.** (1998). Who reads temporal information contained across synchronized and oscillatory spike trains? *Nature.* vol 395, 693-698
5. **Hines, M.L. and Carnevale, N.T.** (2001). NEURON: a tool for neuroscientists. *The Neuroscientist* 7:123-135.
6. **Gilles Laurent and Mohammad Naraghi.** (1994). Odorant-induced Oscillations in the Mushroom Bodies of the Locust. *The Journal of Neuroscience.* 14(5): 2993-3004.
7. **Grunewald B.** (1999). Morphology of feedback neurons in the mushroom body of the honeybee, *Apis mellifera*. *J Comp Neurol.* 1; 404(1):114-26.
8. **Cassenaer S. and Laurent G.** (2007). Hebbian STDP in mushroom bodies facilitates the synchronous flow of olfactory information in locusts. *Nature.* 448, 709-713.